Polymer Chemistry

Accepted Manuscript

This is an *Accepted Manuscript*, which has been through the Royal Society of Chemistry peer review process and has been accepted for publication.

Accepted Manuscripts are published online shortly after acceptance, before technical editing, formatting and proof reading. Using this free service, authors can make their results available to the community, in citable form, before we publish the edited article. We will replace this *Accepted Manuscript* with the edited and formatted *Advance Article* as soon as it is available.

You can find more information about *Accepted Manuscripts* in the Information for Authors.

Please note that technical editing may introduce minor changes to the text and/or graphics, which may alter content. The journal's standard Terms & Conditions and the Ethical guidelines still apply. In no event shall the Royal Society of Chemistry be held responsible for any errors or omissions in this *Accepted Manuscript* or any consequences arising from the use of any information it contains.

ROYAL SOCIETY OF CHEMISTRY

www.rsc.org/polymers

Polymer Chemistry

RSCPublishing

ARTICLE

Synthesis of Multifunctional Poly(1-pyrenemethyl methacrylate)-*b*-Poly(*N*-isopropylacrylamide)-*b*-Poly(*N*-methylolacrylamide)s and Their Electrospun Nanofibers for Metal Ion Sensory Applications

Cite this: DOI: 10.1039/xoxxoooooox

Jau-Tzeng Wang,[1] Yu-Cheng Chiu,[1] Han-Sheng Sun,[1] Kohei Yoshida,[2] Yougen Chen[3] Toshifumi Satoh,[4] Toyoji Kakuchi[2,3,4], and Wen-Chang Chen*[1]*

Received ooth January 2012,
Accepted ooth January 2012,

DOI: 10.1039/xoxxoooooox

www.rsc.org/

We report the synthesis and characterization of multifunctional triblock copolymers, poly(1-pyrenemethyl methacrylate)-*block*-poly(*N*-isopropylacrylamide)-*block*-poly(*N*-methylolacrylamide) (PPy-*b*-PNIPAAm-*b*-PNMA), and their electrospun (ES) nanofibers for thermal and metal-ion detections. The triblock copolymers are composed of fluorescent and metal-ion-sensitive PPy, thermoresponsive PNIPAAm, and chemically crosslinkable PNMA segments. Non-crosslinked ES nanofibers are initially prepared using th
e aforementioned PPy-*b*-PNIPAAm-*b*-PNMA triblock copolymers and followed by thermal crosslinking. It is found that the ES nanofibers prepared from PPy-*b*-PNIPAAm-*b*-PNMA can self-assemble to form nano-scale spherical aggregates with PNMA locating at the core, PNIPAAm at the center layer, and PPy at the shell. This self-assembly nature therefore induces a strong excimer emission between the pyrenyl moieties. Crosslinking process between PNMA blocks is then implemented to stabilize the ES nanofibers since the non-crosslinked ones are metastable objects. The resulting crosslinked nanofibers exhibit predominant wettability and dimension stability under aqueous states, and could perform a detectable photoluminescence transition at different temperatures or toward Fe^{3+} ion. In contrast to its counterpart drop-cast film, the ES nanofibers with a high surface/volume ratio has obviously higher sensing ability toward thermal stimuli and metal ions, which is expected to be applied as multifunctional sensory devices.

Introduction

Multifunctional random or block copolymers containing environmentally responsive segments and fluorescent probes have attracted considerable attention in various sensory applications, such as thermo-, pH-, light-, and chemical-sensitive detections.[1-13] Among them, conjugated rod-coil or coil-coil block copolymers are highly promising ones since the conjugated rod or coil block is highly electronically and optically sensitive and its electronic and optical properties can be readily tuned by the other stimuli-responsive coil block.[14-16] Besides, block copolymers can render self-assembly nanostructures, which provide a versatility for designing sensor devices.[17-22]

For example, Balamurugan et al. reported that poly(thiophene-*g*-*N*-isopropylacrylamide) with fluorescent polythiophene main chain and thermoresponsive poly(*N*-isopropylacrylamide) (PNIPAAm) side chains showed tunable optical properties along with PNIPAAm undergoing a reversible phase transition between 28 and 35 ^{o}C.[23] We reported previously that a rod-coil polyfluorene-*block*-poly(2-(dimethylamino)ethyl methacrylate)) in aqueous solution showed thermo- and pH-dependent photoluminescent (PL) behaviours, in which the polyfluorene (PF) block had been used as an on/off fluorescence indicator.[24] In general, those responsive block copolymers are mainly used in solution state since their efficiency and sensitivity in solution state are substantially superior to those in solid state like spin-coated films. Thus, it remains a challenge to develop solid state devices based on multifunctional block copolymer.

Electrospining is one of the convenient techniques to fabricate nanofibers with a large surface area and tunable morphology.[25-29] The electrospun (ES) nanofibers prepared from functional materials could enhance the sensibility in aqueous solution due to the high surface to volume ratio.[30-34] For example, Okuzaki and coworkers[35] demonstrated that the poly(NIPAAm-*co*-(stearyl acrylate)) ES fibers exhibited reversible and fast volume changes by altering its surrounding temperature, in which the inter-polymer physical crosslinking interaction between SA moieties prevented the ES nanofibers from dissolving in water. Recently, we have succeeded in preparing the ES nanofibers from a triblock copolymer, PF-*b*-PNIPAAm-*b*-poly(*N*-methylolacrylamide) (PF-*b*-PNIPAAm-*b*-PNMA), with a chemically crosslinkable PNMA segment.[31] Upon the crosslinking, of PNMA, the PF-*b*-PNIPAAm-*b*-PNMA nanofibers showed good wettability and integrity in aqueous solution and their photoluminescent (PL) characteristics exhibited a reversible transition when exposed to

different thermal stimulus. Nevertheless, the preparation and applications of ES nanofibers, especially those prepared from mulitfunctional block copolymers, are still limited. Until now, many conjugated polymers bearing specially designed chelating sites have been employed to detecting metal ions; they, however, could hardly achieve the objective for the simultaneous detections towards different stimulus.[36] On the contrary, the block copolymers possessing multiple stimuli-sensitive segments are highly promising to realize the mulitfunctional detections in terms of not only physical stimulus but also chemical ones, based on the one-to-one correspondence between a stimuli-sensitive segment and its related stimuli.

In this study, we report the synthesis and characterization of new poly(1-pyrenemethyl methacrylate)-*b*-PNIPAAm-*b*-PNMA (PPy-*b*-PNIPAAm-*b*-PNMA) triblock copolymers and their ES nanofibers for multi-sensory applications, as shown in Scheme 1. PPy-*b*-PNIPAAm-*b*-PNMA consisted of fluorescent PPy, thermoresponsive PNIPAAm, and chemically cross-linkable PNMA segments, were synthesized by atom transfer radical polymerization (ATRP) method followed by click reaction (scheme 2). Electrospinning technique was utilized to prepare the non-crosslinked ES nanofibers using PPy-*b*-PNIPAAm-*b*-PNMAs and followed by a thermal crosslinking process. The surface structure and inner morphology of the two type ES nanofibers were characterized by scanning electron microscope (SEM) and small-angle X-ray scattering (SAXS), respectively. The relationship between the crosslinked ES nanofiber morphology and its photophysical properties, together with its sensing behaviour in aqueous solution were systematically investigated.

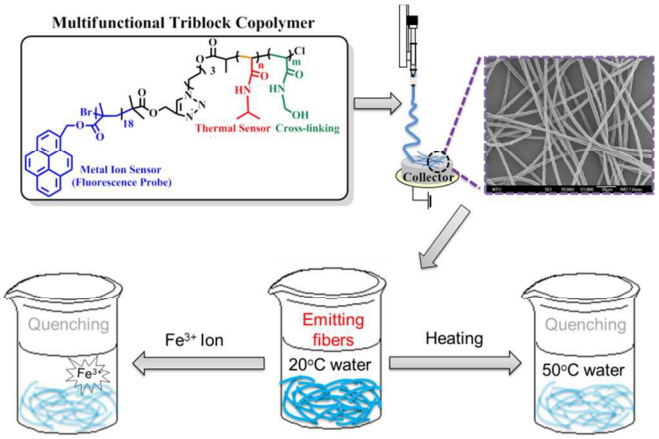

Scheme 1. Design of multifunctional ES nanofibers using PPy-*b*-PNIPAAm-*b*-PNMA triblock copolymers.

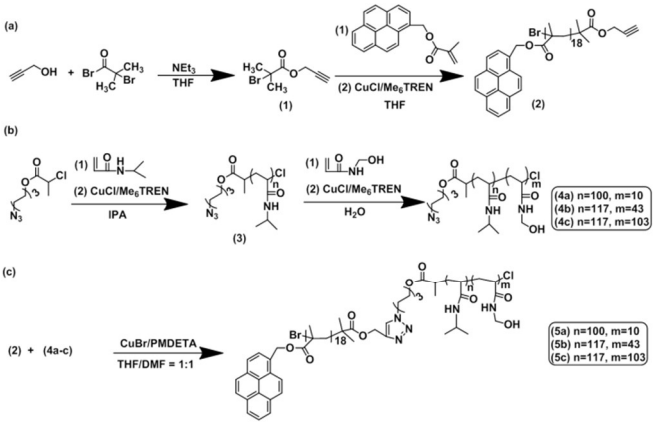

Scheme 2. Synthesis of PPy-*b*-PNIPAAm-*b*-PNMA rod-coil-coil triblock copolymers.

Experimental Section

Materials. *N*-Isopropylacrylamide (NIPAAm) and *N*-methylolacrylamide (NMA) were provided by Tokyo Chemical Industry Co. Japan. NIPAAm was re-crystallized three times from hexane/toluene (10/1, v/v) prior to use. Tris[2-(dimethylamino)ethyl]amine (Me_6TREN) was supplied by Mitsubishi Chemical Co. Japan and distilled under reduced pressure from calcium hydride, and then stored under argon. 1-Pyrenemethyl methacrylate, copper(I) chloride, copper(I) bromide (98%), and *N*,*N*,*N*′,*N*″,*N*″-pentamethyldiethylenetriamine (PMDETA), poly(ethylene oxide) (PEO, M_v = 400,000), propargyl alcohol (99%), and 2-bromoisobutyryl bromide (98%) were purchased from Aldrich Chemical Co. USA and used without further purification. 6-Azidohexyl-2-chloropropanoate (AHCP) was prepared according to our previous report.[31] The propargyl 2-bromoisobutyrate (PBiB, **1**) was synthesized by esterification of propargyl alcohol with 2-bromoisobutyryl bromide.[37] Organic solvents used for syntheses were commercially available and used as received unless otherwise noted.

Synthesis alkynyl-ended poly(1-pyrenemethyl methacrylate) (PPy, 2). 1-Pyrenemethyl methacrylate (1.00 g, 3.33 mmol), CuBr (30.1 mg, 0.210 mmol), PBiB (43.5 mg, 0.21 mmol), and THF (10 mL) were mixed in a Schlenk flask. The mixture was degassed three times using the freeze-pump-thaw cycle. PMDETA (36.4 mg, 0.210 mmol) was then added to the mixture and the flask was immersed in an oil bath at 60 °C for 24 h. The reaction was quenched by exposure to air. The mixture was diluted with THF and the copper species was removed by passing the mixture liquid through a neutral Al_2O_3 column. The light yellow filtrate was concentrated, re-precipitated from ether, collected by filtration, and

dried under vacuum to obtain the polymer product (yield: 70%). ^{1}H NMR in $CDCl_3$, δ (ppm) 0.60-1.00 (2H, -C$\underline{H_2}$-), 1.75-2.0 (3H, -CC$\underline{H_3}$-), 5.00-5.40 (2H, -OC$\underline{H_2}$-), 7.30-7.90 (aromatic $\underline{H}$). $M_{n,GPC\ (THF)}$ = 5,500 g mol^{-1}, M_w/M_n = 1.20.

Synthesis of PPy-*b*-PNIPAAm-*b*-PNMA triblock copolymer (5). Click reaction between alkynyl-ended PPy and azido-ended PNIPAAm-*b*-PNMA blocks was performed according to Scheme 2. Typically, **2** (190 mg, 0.035 mmol), **5b** (300 mg, 0.018 mmol), and CuBr (5.0 mg, 0.035 mmol) were evacuated for 30 min in a Schlenk flask, backfilled with argon, and dissolved with degassed THF/DMF (6 ml, v/v = 1/1). PMDETA (7.3 µl, 0.035 mmol) was then added into the flask. The reaction was performed in a preheated oil bath at 50 ^{o}C for 48 h, and then quenched by exposure to air. After diluted with THF/DMF (volume ratio = 1:1), the copper complex was removed through a silica column. To fully get rid of the unreacted alkynyl-terminated PPy, the obtained product was washed with anisole and dried under vacuum at 50 ^{o}C for 24 h to give the light yellow-green PPy_{18}-*b*-$PNIPAAm_{117}$-*b*-$PNMA_{43}$ (**5b**). Yield, 250 mg (60%). ^{1}H NMR in $CDCl_3$, δ (ppm) 0.91-1.45 (6H, -CH(C$\underline{H_3}$)$_2$), 1.48-1.93 (2H, -C$\underline{H_2}$CH-), 1.94-2.42 (1H, -CH$_2$C$\underline{H}$-), 3.71-3.94 (1H, -C$\underline{H}$(CH$_3$)$_2$), 5.00-5.40 (2H, -OCOC$\underline{H_2}$-), 5.67-6.78 (1H, -CO$\underline{N}$H-), 7.30-7.90 (9H, aromatic $\underline{H}$ of pyrenyl group). ^{1}H NMR in DMSO-d_6, δ (ppm) 0.84-1.18 (6H, -CH(C$\underline{H_3}$)$_2$), 1.25-1.72 (4H, -C$\underline{H_2}$CH-, -C$\underline{H_2}$CH-), 1.80-2.20 (2H, -CH$_2$C$\underline{H}$-, -CH$_2$C$\underline{H}$-), 3.71-3.97 (1H, -C$\underline{H}$(CH$_3$)$_2$), 4.36-4.65 (2H, -NHC$\underline{H_2}$OH-), 5.34-5.63 (1H, -NHCH$_2$O$\underline{H}$), 6.97-7.59 (1H, -CO$\underline{NH}$CH- overlapped with aromatic $\underline{H}$), 7.97-8.42 (1H, -$\underline{NH}$CH$_2$OH). $M_{n,GPC\ (DMF)}$ = 33,000 g mol^{-1}, M_w/M_n = 1.21.

Preparation of Electrospun (ES) Nanofibers and Drop-Cast Films. For preparation of the electrospinning solution, a chloroform solution of PPy_{18}-*b*-$PNIPAAm_{117}$-*b*-$PNMA_{43}$ (**5b**, 90 mg) and PEO (7.2 mg, 8 wt% relative to **5b**) was prepared and stirred for 1 day. The non-crosslinked ES nanofibers were prepared using a single-capillary spinneret, similar to our previous report.[31] The polymer solution was fed into the metallic needle by a syringe pump (KD Scientific Model 100, USA), and maintained the feed rate of 0.2~0.4 ml/h. The tip of metallic needle was connected to a high-voltage power supply (Chargemaster CH30P SIMCO, USA), and maintained at 7 KV during the entire electrospinning process. A collector with a piece of aluminum foil or quartz was placed 10 cm below the tip of the needle to collect ES nanofibers for 5 h. All experiments were carried out at room temperature under a relative humidity of about 40%. For comparison with the ES nanofiber, its counterpart polymer film was drop-cast on a glass substrate from the same polymer solution and dried in an airflow hood.

Characterization. The morphologies of ES nanofibers were recorded by a field-emission scanning electron microscope (FE-SEM, JEOL JSM-6330F) equipped with X-ray micro analysis. The ES nanofibers were sputtered with platinum prior to the images characterization and analysis was operated at an accelerating voltage of 10 kV. Fluorescence optical microscope images were obtained using Two Photon Laser Confocal Microscope (Leica LCS SP5) with a water bath holder. Small-angle X-ray scattering (SAXS) measurements of pure PPy-*b*-PNIPAAm-*b*-PNMA were carried out with graphite-monochromatized Cu KR radiation using a Bruker diffractometer (NanoSTAR Universal System). SAXS data were collected on beamline BL23A1 in the National Synchrotron Radiation Research Center (NSRRC, Taiwan). A monochromatic beam of λ = 0.887 Å was used. The scattering intensity profiles were reported as the plots of the scattering intensity (*I*) *vs.* the scattering vector q, where $q = (4\pi/\lambda)\sin(\theta/2)$, θ is the scattering angle.

The LCST (volume change) of the crosslinked ES nanofibers were carried out on a differential scanning calorimetry (DSC) from TA instrument (TA Q100) with the heating cycle from 20 to 60 ^{o}C at the heating rate of 1.0 ^{o}C/min. The PL spectra of the ES nanofibers and drop-cast films were obtained using a Fluorolog-3 spectrofluorometer (Horiba Jobin Yvon) excited at the wavelength of 350 nm. The crosslinked nanofiber and thin film samples for PL measurements were fixed in cuvettes by adhesive tape and then filled with pure water, as described in our previous study.[30,38] The spectrum in heating or cooling by a temperature control holder was obtained between 20 and 50 ^{o}C with each interval of 10 ^{o}C, in which each specified temperature was fixed for 30 min for each measurement.

Results and discussion

Characterization of polymer structure. The alkynyl-ended poly(1-pyrenemethyl methacrylate) (PPy) was synthesized by ATRP using PBiB as initiator and characterized by GPC and NMR determinations. The characteristic proton resonance signals from monomer repeat units were clearly observed at 7.26 – 8.21, 4.90 – 5.55, 1.55 – 2.12, and 0.42 – 1.16 ppm due to pyrenyl, -CO$_2$CH_2-, -CCH_2-, and methyl groups (Figure S1(a), *SI*). By GPC analysis in Figure S1(b), the molecular weight and molecular weight distribution of the resulting PPy are estimated to be 5,500 g mol^{-1} and 1.20, respectively, from which the monomer repeat units of PPy are estimated to be 18. Click reaction between alkynyl-ended PPy_{18} and N_3-$PNIPAAm_{117}$-*b*-$PNMA_{43}$ was confirmed by GPC, FTIR, and ^{1}H NMR analyses. The GPC spectrum of PPy_{18}-*b*-$PNIPAAm_{117}$-*b*-$PNMA_{43}$ (**5b**, M_n = 33,000 g mol^{-1}; PDI = 1.21, Figure S2(b)) clearly shifts to the high molecular-weight direction in comparison with that of its precursor, N_3-$PNIPAAm_{117}$-*b*-$PNMA_{43}$ (**4b**, M_n = 27,500 g mol^{-1}; PDI = 1.15), suggesting that the click reaction between the hydrophobic PPy and hydrophilic $PNIPAAm_{117}$-*b*-$PNMA_{43}$ blocks is rather successful in binary co-solvent of DMF/THF. In addition, as shown in Figure 1(a), the effective coupling between azido and alkynyl groups is further confirmed by the observation that the characteristic stretching peak of azido group at 2100 cm^{-1} due to **4b** in the FTIR spectrum disappeared completely after click reaction with PPy. The ^{1}H NMR spectra of the PPy_{18}-*b*-$PNIPAAm_{117}$-*b*-$PNMA_{43}$ (**5b**) in $CDCl_3$ is shown in Figure 1(b), from which the proton signals due to PPy and PNIPAAm blocks clearly appear, while the proton signals due to the hydrophilic PNMA block cannot be observed due to its limited solubility in $CDCl_3$. For this reason, another hydrophilic *d*-solvent, DMSO-d_6, was employed to further carry out the ^{1}H NMR measurements, as shown in Figure 1(c). In this case, the proton signals at *d* (3.7 – 4.1 ppm), *e* (4.3 – 4.7 ppm), *f* (5.2 – 5.6 ppm), *g*

(7.0 – 7.5 ppm), and *h* (8.0 – 8.5 ppm) due to the hydrophilic PNIPAAm and PNMA blocks can be clearly seen, while those from PPy block vanish due to their poor solubility in DMSO-d_6.[38,39] It seems difficult to find a suitable deuterated reagent for the ^{1}H NMR measurements. Similarly, **5a** (M_n = 18,000 g mol^{-1}, PDI = 1.21) and **5c** (M_n = 47,000 g mol^{-1}, PDI = 1.32) with respective block compositions of PPy_{18}-*b*-$PNIPAAm_{100}$-*b*-$PNMA_{10}$ and PPy_{18}-*b*- $PNIPAAm_{117}$-*b*-$PNMA_{103}$ are also fully characterized

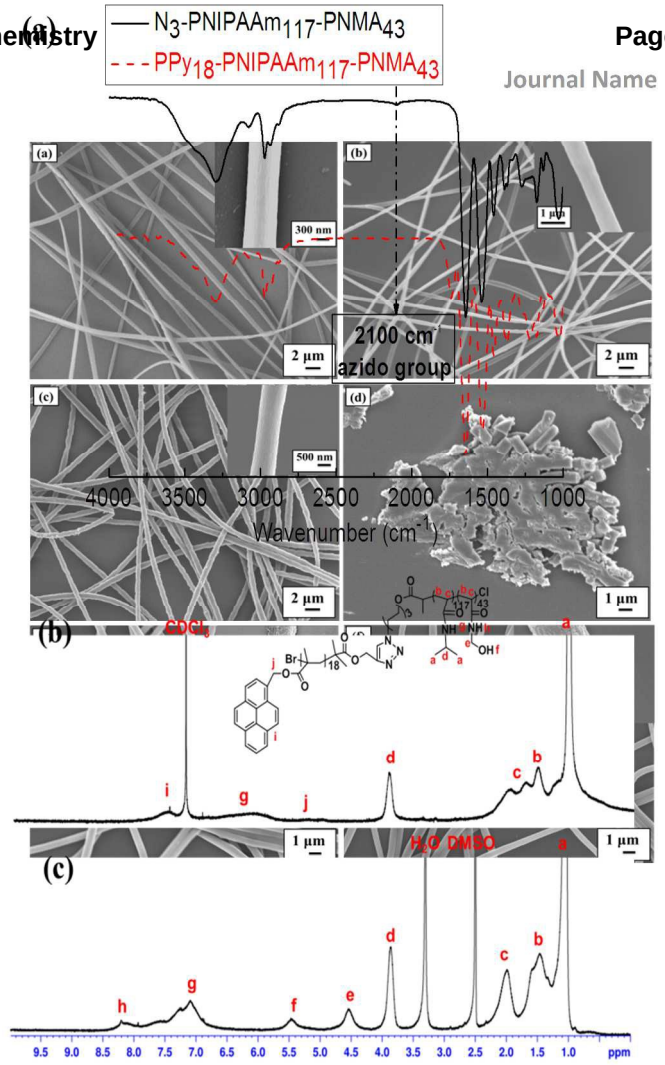

Figure 1. (a) IR spectra of N_3-$PNIPAAm_{117}$-*b*-$PNMA_{43}$ (**4b**) and PPy_{18}-*b*-$PNIPAAm_{117}$ -*b*-$PNMA_{43}$ (**5b**) and ^{1}H-NMR spectra of PPy_{18}-*b*-$PNIPAAm_{117}$-*b*-$PNMA_{43}$ (**5b**) in $CDCl_3$ (b) and in DMSO (c).

by GPC, FTIR, and ^{1}H NMR analyses, as shown in Figures S2, S3, and S4. Besides, from DSC measurements in Figure S6 the glass transition temperatures (T_gs) of **5a**, **5b**, and **5c** are estimated to be 128, 135, and 140 °C, respectively.

Electrospun Nanofibers Prepared from PPy-*b*-PNIPAAm-*b*-PNMA. For electrospinning process, a small amount of high molecular-weight poly(ethylene oxide) (PEO, M_v = 400,000 g mol^{-1}) was blended with **5** to enhance the solution viscosity because the diverse polarity of each block and the relative low molecular weight of PPy-*b*-PNIPAAm-*b*-PNMA result in insufficient entanglement in chloroform solution. Note that the PEO can be extracted away by water after the PNMA blocks are cross-linked by thermal curing. Figure 2 shows the SEM images of the non-cross-linked ES nanofibers prepared from the chloroform solution of PEO/**5** blend (PEO, 8 wt% relative to **5**). The diameters of the **5a**, **5b** and **5c** ES nanofibers before removing PEO are 740 ± 79, 810 ± 68, and 890 ± 55 nm, respectively. The increased average diameter from 740 to 890 nm is considered to be due to the increasing molecular weight from **5a** to **5c**.[40] The as-spun nanofibers were then thermo-cured at 100 °C for 48 h in a vacuum oven in order to crosslink the PNMA blocks through the formation of bis(methylene ether) by loss of water and formaldehyde molecules.[41] After crosslinking process, the nanofiber mats were washed with water for about 5 times at 30 °C to remove PEO and then dried at the same temperature under vacuum. It is observed that the crosslinked **5b** and **5c** ES nanofibers (Figure 2(e) and (f)) maintain a stable fiber shape with rougher surface and their diameters reduce to 705 ± 58 and 784 ± 85 nm, respectively, compared to their corresponding non-crosslinked ones. Note that the average fiber diameter was estimated based on a statistical average of fifty fibers for each sample. In contrast, the crosslinked **5a** nanofibers cannot effectively resist the water extraction due to the insufficient cross-linking between PNMA blocks, eventually leading to a thin-film-like object in Figure 2(d). Thus, the further discussion on the crosslinked **5a** is neglected. It seems clear that the waterproof ability of the cross-linked ES nanofibers significantly depends on the length of the cross-linkable PNMA segment.

Figure 2. FE-SEM images of non-crosslinked ES nanofibers from PEO/**5** chloroform solution (100 mg/ml): (a) PEO/**5a**,(b) PEO/**5b** and (c) PEO/**5c**, and their cross-linked ES nanofibers: (d) **5a**, (e) **5b** and (f) **5c**.

The inner morphologies of the crosslinked **5b** and **5c** nanofibers are investigated by SAXS. For discussion on the crosslinked **5b** ones, the as-cast **5b** bulk sample prepared from the original ES polymer solution is cross-linked after solvent evaporation as a control experiment and used to inspect the solvent-induced self-assembly behaviour of amphiphilic triblock copolymers. Figure 3(a) shows the SAXS pattern of the crosslinked **5b** bulk sample. Given that the crosslinking temperature at 100 °C is much lower than T_g, it is reasonable to assume that the inner structure of the crosslinked **5b** bulk sample keeps the same with that in chloroform solution. The spectrum of the crosslinked **5b** bulk sample observed in Figure 3(a) shows a diffraction pattern of 1 : √2 : √3 : √4 : √5, suggesting the formation of a body-center cubic (BCC) structure with a domain space of 23.3 nm that is estimated from the first-order peak at q = 0.027 Å. Note that the high-order diffraction peaks (√3 , √4 , and √5) become broader probably because the obtained triblock copolymer has a slightly larger molecular weight distribution (PDI : 1.21). In comparison to the **5b** bulk sample, the SAXS results of the crosslinked **5b** nanofibers only show a first-order peak with a *d*-spacing of 19 nm (Figure 3(b)), which indicates the formation of a random spherical nanostructure with a smaller domain size. It is probably resulted from the rapid evaporation of solvent and strong shear force provided by the electric filed during the ES process. Similar results have also been observed for the crosslinked **5c** nanofibers, which have a larger domain spacing of 25.1 nm due to its higher volume fraction of the PNMA block. The formation of such nano-spherical aggregates in the crosslinked bulk sample or nanofibers can be basically attributed to the preparation method of the ES polymer solution. In greater detail, chloroform used for preparing ES polymer solution is a poor solvent for PNMA block but a good solvent for both PPy and PNIPAAm blocks. This characteristic therefore leads to the intermolecular aggregation and the eventual formation of the nano-spheres with the PNMA locating at the core, PNIPAAm at the center layer, and PPy at the outer layer as illustrated in Figure 3(c). Obviously, a larger *d*-spacing would be rationally obtained with increasing PNMA length.

Thermo-responsive characteristics of the crosslinked ES nanofibers. The LCSTs of the triblock copolymers are first investigated. The optical transmittance-*versus*-temperature measurements of 1 mg ml^{-1} **5a-5c** aqueous solutions are used to evaluate the LCSTs of these triblock copolymers (Figure 4(a)), from which the LCSTs of **5a-5c** in water are 32.5, 37.0, and 40.0 °C, respectively. The higher LCST is due to the longer hydrophilic PNMA block length since a hydrophilic block incorporated to PNIPAAm would enhance the LCST of the entire block copolymer. Differently form the LCST measurements for triblock copolymers, the LCSTs of the crosslinked ES nanofibers in water are evaluated by the DSC measurement. The endothermic peaks in Figure 4(b-c) indicate the dissociation of the hydrogen-bonding between PNIPAAm block and water molecules as the temperature is enhanced. The LCST of the crosslinked **5b** and **5c** ES nanofibers are 32.1 and 37.9 °C, respectively, both of which are lower than those in their aqueous solutions, due to the crosslinking effect caused by the PNMA blocks. To observe the temperature-induced

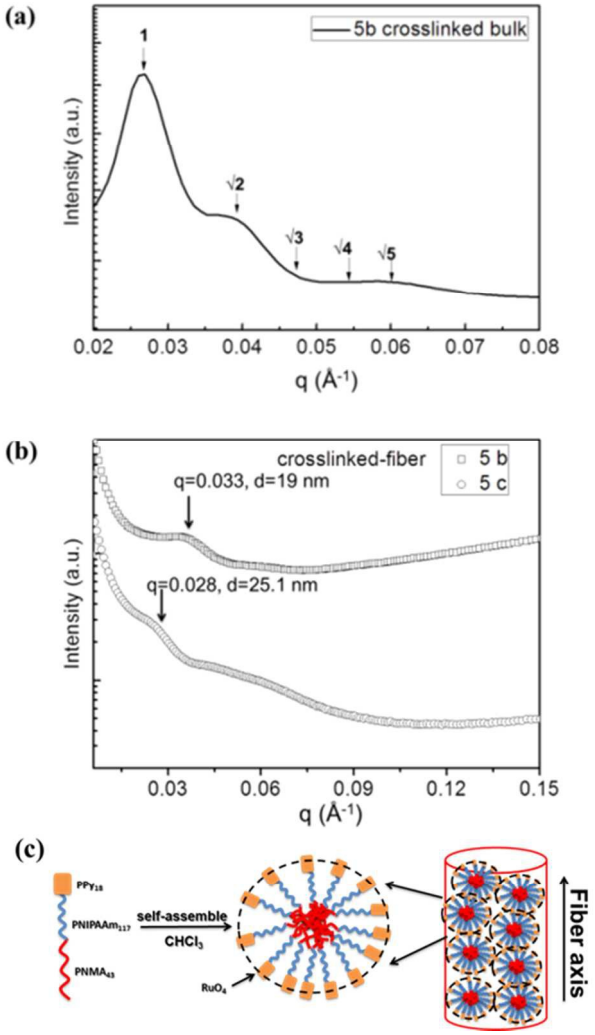

volume changes

Figure 3. SAXS data of (a) **5b** crosslinked bulk sample and (b) **5b** and **5c** crosslinked fibers; and (c) Illustration of the interior morphology of **5b** crosslinked ES nanofibers.

of the cross-linked nanofibers, the samples are prepared followed by our previous reports for the SEM analyses.[30,31] The morphologies of the crosslinked **5b** and **5c** ES nanofibers in water under different temperatures are shown in Figure 5. When the surrounding temperature is kept at 20 °C (below LCST), the crosslinked **5b** nanofibers in water maintains the cylindrical shape, while show a swollen morphology with a diameter of 790 ± 58 nm. Upon rising temperature to 50 °C, its diameter reduces to 610 ± 49 nm and it obviously has a shrinking and more compact morphology, which is considered to be caused by the coil-globule transition of PNIPAAm chains during the hydrogen-bonding dissociation process.[31] In the case of the crosslinked **5c** nanofibers prepared from **4c** with a longer PNMA block (Figure S7), they show only a

slight swelling/shrinking effect (815 ± 35 nm/785 ± 25 nm) at 20 and 50 °C, respectively, compared with the situation in the crosslinked **5b** nanofibers. This result can be reasonably attributed to the fact that the crosslinked **5c** nanofibers have much higher crosslinking volume fraction, which limits the chain mobility and thus weakens the swelling/shrinking effect. Therefore, the cross-linked **5b** ES nanofibers are mainly used to carry out sensory detections.

Thermo-responsivity of the cross-linked ES nanofibers. Figures 5c and 5d show the dependence of the PL intensity of the crosslinked **5b** ES nanofibers on temperature in the heating/cooling cycles between 20 and 50 °C. The PL spectra of the ES nanofibers exhibit the main emission peak at 475 nm, which comes from the strong excimer emission induced by the aggregation of PPy block in water. For the cross-linked **5b** nanofibers, a continuous quenching of PL intensity is observed in Figure 5(c) as the temperature is gradually increased from 20 to 50 °C. The PL quenching turns out to be reversible as shown in Figure 5(d) as the cooling process from 50 to 20 °C can recover the emission intensity to the original value. The change in the emission intensity as a function of temperature is shown in Figure S8, where exhibited a 1.5~1.7-fold variation by comparing the intensities at 20 and 50 °C. The dependence of the PL intensity on temperature can be ascribed to the temperature-induced coil-globule-coil transition of the thermo-responsive PNIPAAm block, i.e. the PNIPAAm chains under a temperature above LCST would undergo a coil-to-globule transition leading to a collapsed compact conformation, which blocks the effective excitation absorption and therefore causes a PL quenching effect. On the other hand, the PNIPAAm block under a temperature below LCST takes a loose coil conformation, which makes the crosslinked **5b** nanofibers swell in water and optically transmittable, thus resulting in the normal excitation and PL emission.[42] These results are well coincident with the aforementioned volume changes observed for these cross-linked nanofibers by SEM observations under different temperatures. The PL intensity of the crosslinked **5b** nanofibers at 20 °C is about 3.3 × 10^6 while that at 50 °C is only 1.8 × 10^6, from which a 45% decrement is known during the heating process. As a comparison, **5b** thin film only shows a 15% decrement during the same heating process. It is rather obvious that the crosslinked **5b** nanofibers own a superior thermo-responsivity than its counterpart drop-cast films because the ES nanofibers have a much higher surface-to-volume ratio. Similar results are obtained for the crosslinked **5c** nanofibers though they have a much longer PNMA block, as shown in Figure S9**.** The crosslinked **5c** nanofibers behave very similarly in morphology and PL intensity changes with those of the cross-linked **5b** nanofibers during the heating/cooling cycles. However, the degree of these changes is much lower than that of **5b** nanofibers perhaps because the chain movement in the highly cross-linked **5c** nanofibers has been to a greater extent restricted. It suggests that the thermoresponsivity of the cross-linked nanofibers would become weaker when the crosslinking effect is too strong. Similarly to the cross-linked **5b** nanofibers, the crosslinked **5c** nanofibers also perform much better in thermoresponsivity than their counterpart thin films. The reversibility and time-dependent PL change for the crosslinked **5b** nanofibers were then tested. As shown in Figure 6, the cross-linked **5b** nanofibers exhibit moderate responsivity toward thermal stimulus and rather stable on-off switching property in the PL-Time curves. In addition, the real-time images for the reversibility measurements were recorded by laser confocal microscope, in which the crosslinked **5b** nanofibers were immersed in a water-filled incubator. The cylindrical cross-linked **5b** nanofibers show an apparent PL emitting and quenching transition with temperature switching between 20 and 50 °C, as shown in Figure 6(b) and (c).

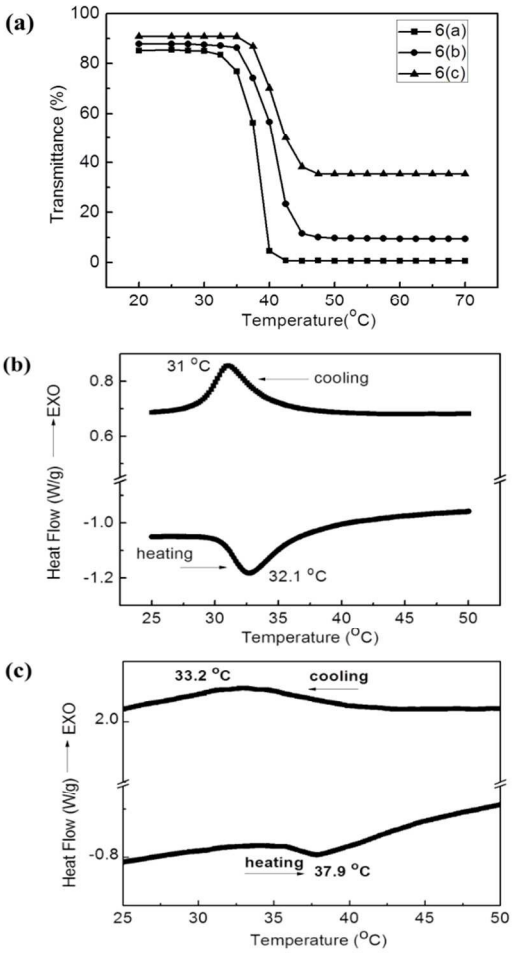

Figure 4. (a) Optical transmittance dependence of PPy-*b*-PNIPAAm-*b*-PNMA **(5a-c)** aqueous solution on temperature and

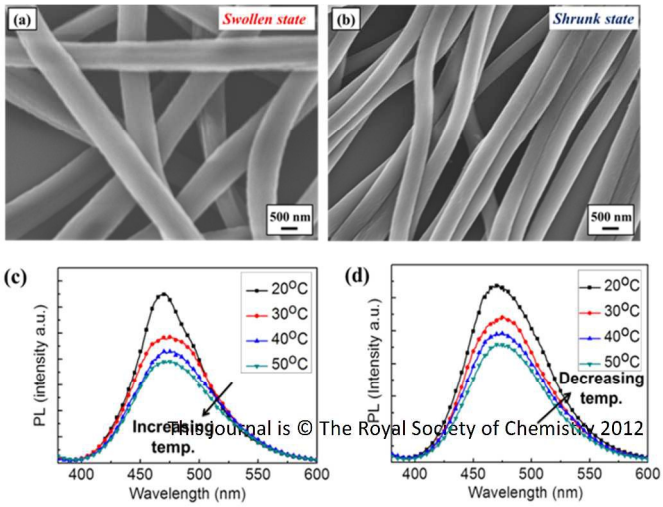

DSC thermograms of cross-linked ES nanofibers: (b) **5b** and (c) **5c**.

Figure 5. FE-SEM images of the crosslinked **5b** nanofibers in water under temperatures: (a) 20 °C and (b) 50 °C; PL spectra of the cross-linked **5b** ES nanofibers with: (c) increasing temperature from 20 to 50 °C and (d) decreasing temperature from 50 to 20 °C.

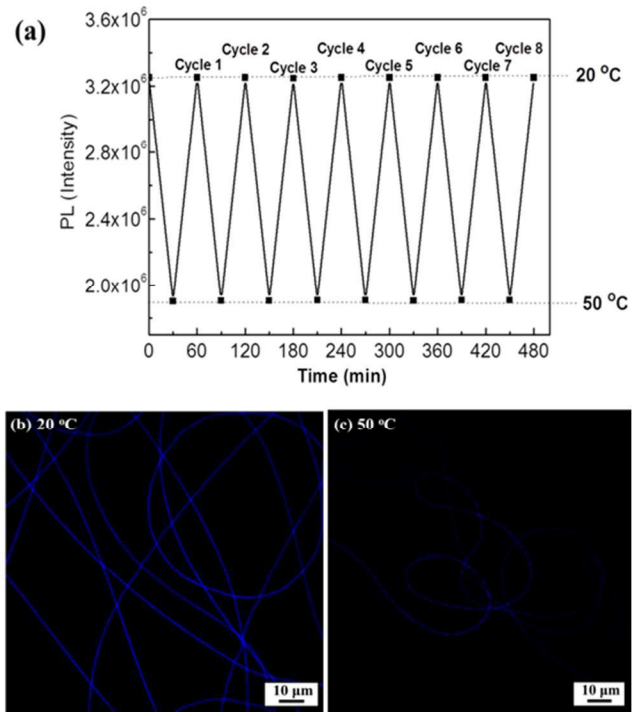

Figure 6. (a) Reversibility of time-dependent "on-off-on" fluorescence intensity profile of the crosslinked **5b** nanofibers; and confocal images of the cross-linked **5b** nanofibers immersed in pure water at (b) 20 °C and (c) 50 °C.

Metal Ion Sensing behaviour of the cross-linked ES nanofibers. It has been reported that the pyrene moiety can be used to recognize some heavy metal ions.[43] Given that both of the triblcok copolymers and their cross-linked nanofibers have PPy ingredients, their sensing behaviours toward metal ions have been investigated in this study. The fluorescent behaviour of **5a** toward different metal ions is shown in Figure 7, in which the I_0 and I stand for the fluorescence intensities at 475 nm in the absence and presence of each metal ion, respectively. Compared to other metal ions such as K^+, Pb^{2+}, Ni^{2+}, Mg^{2+}, and Mn^{2+}, the photoluminescence of **5a** has been significantly quenched upon adding Fe^{3+} and Hg^{2+} to its aqueous solution, leading to the sensing possibility for the two metal ions. The reason for such luminescence quenching can be explained as follows: the energy barrier for filling the empty electronic orbits of Fe^{3+} and Hg^{2+} matches very well with that for the electronic transition of PPy from its excited state to its basic state, which leads to the absorption of excited PPy electrons by Fe^{3+} and Hg^{2+} and the luminescence quenching phenomenon.[43]

The fluorescent responses of the crosslinked **5b** ES nanofibers and their thin film toward Fe^{3+} in aqueous solution with different concentrations ($C(Fe^{3+})$) are shown in Figure 8. It can be seen that the fluorescence intensity decreases steadily with increasing $C(Fe^{3+})$ for both cases. Nevertheless, the cross-linked **5b** ES nanofibers with large surface area show a significantly higher sensitivity for recognizing Fe^{3+}, i.e. luminescence is quenched down to a value of about 85% relative to initial one in the presence of Fe^{3+} at $C(Fe^{3+}) = 2 \times 10^{-5}$ M and this value can goes down to

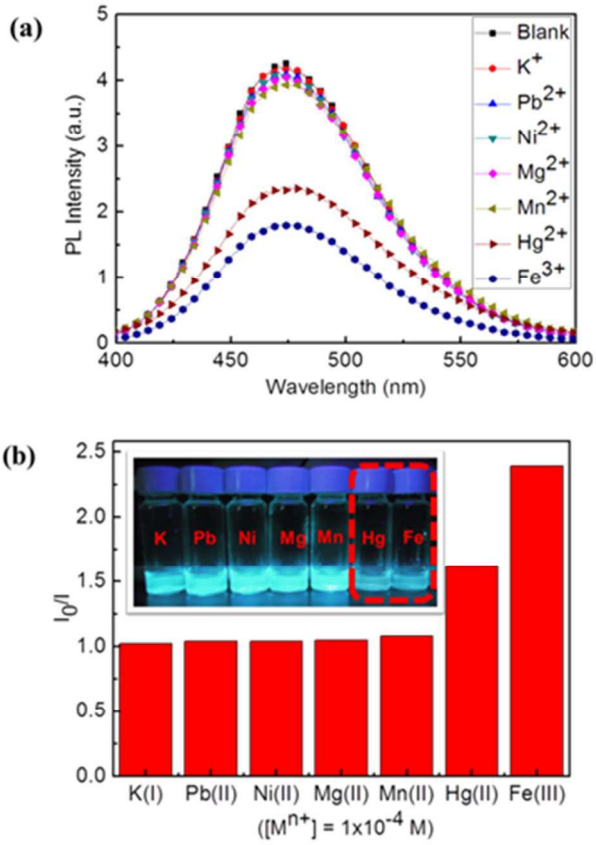

50% when $C(Fe^{3+})$ increases to 10^{-4} M.

Figure 7. (a) PL spectra and (b) relative PL intensity histogram of **5a** aqueous solution in present of different metal ions at a concentration of 10^{-4} M.

In contrast, the quenching degree for the **5b** thin film can hardly reach 15% unless the $C(Fe^{3+})$ is risen up to ~10^{-2} M. The I_0/I-$C(Fe^{3+})$ relationship for both cases are summarized in Figure 8(c), which clearly indicates that the sensibility of the cross-linked **5b** ES nanofibers is significantly higher than that of the **5b** thin film by 3 orders. It suggests that the cross-linked nanofibers with much larger surface/volume ratio accelerate the diffusion of Fe^{3+} from aqueous solution to the PPy blocks confined within nanofibers. This phenomenon has been directly observed in the real-time confocal microscopy (Figure 9), by which it can be seen that the crosslinked **5b** ES nanofibers in pure water at 20 °C reveal a strong blue emission, whereas the luminescence diminishes quickly once Fe^{3+} is added.

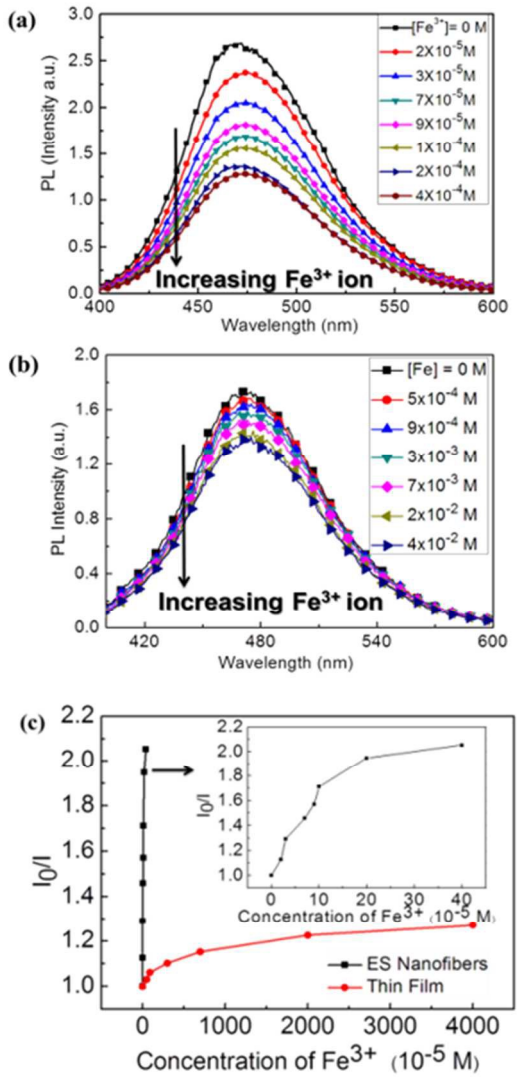

Figure 8. PL dependence on $C(Fe^{3+})$: (a) crosslinked **5b** ES nanofibers and (b) drop-cast **5b** thin films; and (c) Stern-Volmer plots (I_0/I dependence) of the same nanofibers and thin films on $C(Fe^{3+})$ measured at 475 nm. Inset: Stern-Volmer plots of the cross-linked **5b** ES nanofibers on $C(Fe^{3+})$ from 0 to 4.0 × 10^{-4} M.

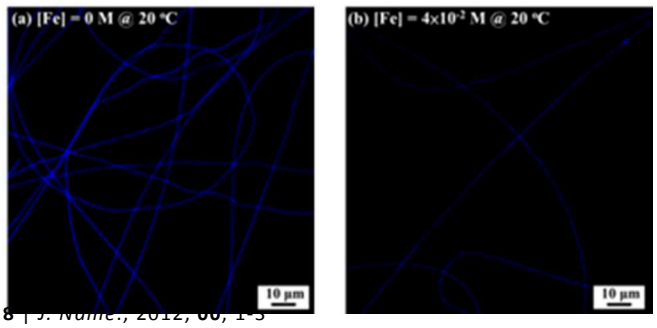

Figure 9. Confocal images of the crosslinked **5b** nanofibers immersed in pure water at 20 °C and (a) $C(Fe^{3+})$ = 0 M and (b) $C(Fe^{3+}) = 4.0\times10^{-2}$ M.

For more detailed clarification, the iron distribution in the cross-linked **5b** ES nanofibers is examined by EDS. The nanofibers deposited on silicon substrate was immersed in Fe^{3+} aqueous solution at $C(Fe^{3+})$ = 0.4 mM for 20 min and then washed with pure water for 30 min to remove the free metal ions., The carbon and iron mapping images in Figure 10(a-c) indicate that Fe^{3+} are only effectively captured by the **5b** cross-linked nanofibers since no iron species are left on substrate as the dark region shown. The iron content within the crosslinked **5b** ES nanofibers is 5.36 atom% estimated from EDX spectrum (Figure 10(d)).

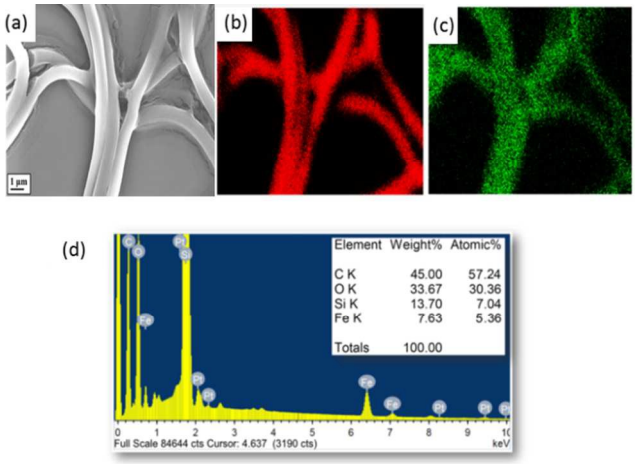

Figure 10. (a) FE-SEM images of the **5b** crosslinked nanofibers in the presence of Fe^{3+}, (b) & (c) EDS maps of **C** and **Fe** elements within the confined area in (a), and (d) EDS spectrum recorded within the region in (a).

Conclusions

We have successfully prepared the fluorescent PPy-*b*-PNIPAAm-*b*-PNMA triblock copolymers and their electrospun nanofibers. The triblock copolymer, PPy-*b*-PNIPAAm-*b*-PNMA, self-assembles to form nano-sphere aggregates with the PNMA locating at the core, PNIPAAm at the center layer, and PPy at the shell. By precisely controlling the repeat units of thermal crosslinkable PNMA block, the prepared electrospun nanofibers show the outstanding wettability and integrity in aqueous solution. The crosslinked block copolymer (**5b** film presents an orderly BCC structure while the corresponding nanofibers show random sphere morphology with smaller domain size of 19 nm due to the rapid solvent evaporation during electrospinning. In comparison to the drop-cast thin film, the cross-linked nanofibers with high surface/volume ratio significantly enhance the sensitivity toward stimulus of temperature and metal ions. The PL emitting/quenching switching of the cross-linked nanofibers in a temperature range of 20 - 50 °C turns out to

be reversible. In addition, the blue emission of nanofibers can be remarkably quenched by Fe^{3+} even when the $C(Fe^{3+})$ is down to 10^{-5} M, suggesting that the crosslinked nanofibers is possible a metal-ion-sensory device. Overall, we achieve the multifunctional detections in terms of temperature and metal ions like Fe^{3+} and Hg^{2+} using the PPy-*b*-PNIPAAm-*b*-PNMA-made cross-linked nanofibers.

Acknowledgment

We gratefully acknowledge the National Science Council of Taiwan for the financial support, and the staffs of Technology Commons, College of Life Science, NTU for help with [the confocal laser scanning microscopy (CLSM)]. K. Yoshida, Y.-G. Chen, T. Satoh, and T. Kakuchi thank the financial support by the MEXT (Japan) program "Strategic Molecular and Materials Chemistry through Innovative Coupling Reactions" of Hokkaido University.

Notes and references

[1] Department of Chemical Engineering, National Taiwan University, Taipei, 10617, Taiwan, [2] Graduate School of Chemical Sciences and Engineering, Graduate School of Engineering, Hokkaido University, Sapporo 060-8628, Japan, [3] Frontier Chemistry Center, Graduate School of Engineering, Hokkaido University, Sapporo 060-8628, Japan, and [4] Division of Biotechnology and Macromolecular Chemistry, Graduate School of Engineering, Hokkaido University, Sapporo 060-8628, Japan

Corresponding authors: W. C. Chen (chenwc@ntu.edu.tw), T. Kakuchi (kakuchi@poly-bm.eng.hokudai.ac.jp)

† Electronic Supplementary Information (ESI) available: The synthesis of PBiB initiator, polymerization conditions, and molecular weights of N_3-PNIPAAm-*b*-PNMA (**4a, 4b, 4c**) diblock copolymers, GPC profiles of copolymers, **2**, **4a**, **4b**, **4c, 5a**, **5b**, and **5c**, ^{1}H NMR spectra of polymers, **2**, **4a**, **4c**, **5a, 5c**, IR spectra of copolymers, **4a**, **4c, 5a**, **5c**, DSC curves of copolymers, **5a**-**5c.** FE-SEM images of **5b** and **5c**, and photoluminescence spectra of cross-linked ES nanofibers **5c** and drop casting films **5b** and **5c** are available. See DOI: 10.1039/b000000x/

(1) J. Hu, C. Li, S. Liu, *Langmuir* **2010**, *26*, 724-729.
(2) X. Zhou, F. Su, W. Gao, Y. Tian, C. Youngbull, R. H. Johnson, D. R. Meldrum, *Biomaterials* **2011**, *32*, 8574-8683.
(3) S. W. Thomas, G. D. Joly, T. M. Swager, *Chem. Rev.* **2007**, *107*, 1339-1386.
(4) F. Liu, M. W. Urban, *Prog. Polym. Sci.*, **2010**, *35*, 3-23.
(5) X. Yang, J. J. Grailer, I. J. Rowland, A. Javadi, S. A. Hurely, V. Z. Matson, D. A. Steeber, S. Ging, *Acs Nano* **2010**, *4,* 6805-6817.
(6) W. C. Wu, Y. Tian, C. Y. Chen, C. S. Lee, Y. J. Sheng, W. C. Chen, A. K. Y. Jen, *Langmuir* **2007**, *23*, 2805-2814.
(7) J. You, J. A. Yoon, J. Kim, C. F. Huang, K. Matyjaszewski, E. Kim, *Chem. Mater.*, **2010**, *22*, 4426-4434.
(8) K. Iwai, Y. Matsumura, S. Uchiyama, A. P. de silva, *J. Mater. Chem.* **2005**, *15*, 2796-2800.
(9) D. Wang, R. Miyamoto, Y. Shiraishi, T. Hirai, *Langmuir* **2009**, 25, 13176-13182.
(10) A. Nagai, K. Kokado, J. Miyake, Y. Cyujo, *J. Polym. Sci., Part A: Polym. Chem.,* **2010**, *48*, 627-634.
(11) L. N. Chen, Y. C. Chiu, J. J. Hung, C. C. Kuo, W. C. Chen, *Macromol. Chem. Phys.* **2014**, *215*, 286-294.
(12) J. Hu, C. Li, S. Liu, *Langmuir* **2010**, 26, 724-729.
(13) X. Wan, T. Liu, S. Liu, *Langmuir* **2011**, 27, 4082-4090.
(14) J. J. Li, J. J. Wang, Y. N. Zhou, Z. H. Luo, *RSC Adv.* **2014**, *4*, 19869-19877.
(15) A. D. Cuendias, R. C. Hiorns, E. Cloutet, L. Vignau, H. Cramail, *Polym. Int.* **2010**, *59*, 1452-1476.
(16) C. Osuji, C. Y. Chao, I. Bita, C. K. Ober, E. L. Thomas, *Adv. Funct. Mater.* **2002**, *12*, 753-758.
(17) K. K. Huang, Y. K. Fang, J. C. Hsu, C. C. Kuo, W. E. Chang, W. C. Chen, *J. Polym. Sci., Part A: Polym. Chem.,* **2011**, *49* 147-155.
(18) J. Liu, L. Song, X. Zhang, X. Li, *J. Polym. Sci., Part B: Polym.Phys.,* **2014**, *52*, 953-959.
(19) H. Ahn, S. Y. Kim, O. Kim, I. Choi, C. H. Lee, J. H. Shim, M. J. Park, *Acs Nano* **2013**, *7*, 6162-6169.
(20) J. Hu, X. Zhuang, L. Huang, L. Lang, X. Chen, Y. Wei, X. Jing, *Langmuir* **2008**, *24*, 13376-13382.
(21) Y. Mai, A. Eisenberg, *Chem. Soc. Rev.* **2012**, *41*, 5969-5985.
(22) C. L. Liu, C. H. Lin, C. C. Kuo, S. T. Lin, W. C. Chen, *Prog. Polym. Sci.* **2011**, *36*, 603-712.
(23) S. S. Balamurugan, G. B. Bantchev, Y. M. Yang, R. L. Mccarley, *Angew. Chem. Int. Ed.,* **2005**, *44*, 4872-4876.
(24) S. T. Lin, Y. C. Tung, W. C. Chen, *J. Mater. Chem.* **2008**, *18*, 3985-3992.
(25) S. Mahalingam, M. Edirisinghe, *Macromol. Rapid Commun.*, **2013**, *34*, 1134-1139.
(26) Y. Yao, L. Zhao, J. Yang, J. Yang, *Biomacromolecules* **2012**, *13*, 1837-1844.
(27) D. H. Reneker, I. Chun, *Nanotechnology* **1996**, *7*, 216-223.
(28) D. Li, Y. Xia, *Adv. Mater.* **2004**, *16*, 1151-1170.
(29) S. K. Chae, H. Park, J. Yoon, C. H. Lee, D. J. Ahn, J. M. Kim, *Adv. Mater.* **2007**, *19*, 521-524.
(30) Y. C. Chiu, C. C. Kuo, J. C. Hsu, W. C. Chen, *ACS Appl. Mater. Interfaces.***2010**, *2*, 3340-3347.
(31) Y. C. Chiu, Y. Chen, C. C. Kuo, J. C. Hsu, S. H. Tung, T. Kakuchi, W. C. Chen, *ACS Appl. Mater. Interfaces.* **2012**, *4*, 3387-3395.
(32) J. H. Syu, Y. K. Cheng, W. Y. Hong, H. P. Wang, Y. C. Lin, H. F. Meng, H. W. Zan, S. F. Horng, G. F. Chang, C. H. Hung, Y. C. Chiu, W. C. Chen, M. J. Tsai, H. Cheng, *Adv. Funct. Mater.* **2013**, *23*, 1566-1547.
(33) L. N. Chen, C. C. Kuo, Y. C. Chiu, W. C. Chen, *RSC Adv.* **2014**, *4*, 45345-45353.
(34) M. Wang, G. Meng, Q. Huang, Y. Qian, *Environ. Sci. Technol.* **2012**, 46, 367-373.
(35) H. Okuzaki, K. Kobayashi, H. Yan, *Macromolecules* **2009**, *42*, 5916-5918.
(36) Y. Bao, H. Wang, Q. Li, B. Liu, Q. Li, W. Bai, B. Jin, R. Bai, *Macromolecules* **2012**, *45*, 3394-3401.
(37) G. D. Fu, L. Q. Xu, F. Yao, K. Zhang, X. F. Wang, M. F. Zhu, S. Z. Nie, *ACS Appl. Mater. Interfaces.* **2009**, *2*, 239-243.

(38) W. Zhang, X. Jiang, Z. He, D. Xiong, P. Zheng, Y. An, L. Shi, *Polymer* **2006**, *47*, 8203-8209.
(39) C. R. Heald, S. Stolnik, K. S. Kujawinski, C. De Matteis, M. C. Garnett, L. Illum, S. S. Davis, S. C. Purkiss, R. J. Barlow, P. R. Gellert, *Langmuir* **2002**, *18*, 3669-3675.
(40) A. Greiner, J. H. Wendorff, *Angew. Chem. Int. Ed.* **2007**, *46*, 5670-5703.
(41) N. R. Brown, C. E. Frazier, *Int. J. Adh. Adh.* **2007**, *27*, 547-553.
(42) Y. Y. Li, X. Z. Zhang, H. Cheng, G. C. Kim, S. X. Cheng, R. X. Zhuo, *Biomolecules*, **2006**, *7*, 2956-2960.
(43) S. H. Lee, J. Kumar, S. K. Tripathy, *Langmuir* **2000**, *16*, 10482-10489.

For Table of Contents Graphical Abstract Use Only

Synthesis of Multifunctional Poly(1-pyrenemethyl methacrylate)-*b*-Poly(*N*-isopropylacrylamide)-*b*-Poly(*N*-methylolacrylamide)s and Their Electrospun Nanofibers for Metal Ion Sensory Applications

Jau-Tzeng Wang,[1] Yu-Cheng Chiu,[1] Han-Sheng Sun,[1] Kohei Yoshida,[2] Yougen Chen[3] Toshifumi Satoh,[4] Toyoji Kakuchi[2,3,4], and Wen-Chang Chen*[1]*

Poly(1-pyrenemethyl methacrylate)-*block*-poly(*N*-isopropylacrylamide)-*block*-poly(*N*-methylolacrylamide) triblock copolymers were employed to fabricate multifunctional electrospun (ES) nanofibers, which were used to detect thermal and metal-ion with a high sensitivity.